

# COLD ADAPTATION MECHANISMS OF ASPARTATE TRANSCARBAMOYLASE FROM *GLACIIBACTER SUPERSTES*, AN ARCTIC PSYCHROPHILIC BACTERIUM

ANTONIO MONDINI<sup>1</sup>, GEORGIANA NECULA-PETRAREANU<sup>1</sup>, VICTORIA IOANA PAUN<sup>1</sup>,  
LAVINIA IANCU<sup>1</sup> AND CRISTINA PURCAREA<sup>1</sup>

Structural analyses of the aspartate transcarbamoylase (ATCase) from *Glaciibacter superstes*, a psychrophilic bacterium isolated from an Alaska ice wedge, highlighted relevant molecular adaptations to cold environments of the key enzyme catalyzing the first step of the pyrimidine *de novo* biosynthetic pathway. In comparison with mesophilic and thermophilic homologues, the amino acid sequence of the catalytic subunit of this cold-active enzyme was characterized by the complete absence of cysteine residues, a reduced incidence of glutamate and lysine and a higher representation of aspartate and arginine residues, alongside a higher content of coils in the secondary structure. Moreover, a major difference in the distribution of both hydrophobic and hydrophilic clusters along the psychrophilic enzyme was observed as compared to mesophilic and hyperthermophilic counterparts. Comparison of the *G. superstes* ATCase sequence with that of the psychrophilic *Cryobacterium sp.* corroborated the proposed cold adaptation pattern. These structural features of the *G. superstes* ATCase appeared to confer a higher flexibility and ability for catalysis at low temperatures, confirming general thermal adaptation strategies found in enzymes from microorganisms thriving in cold environments.

**Keywords:** aspartate transcarbamoylase, extremophiles, cold-active enzymes, structure.

## INTRODUCTION

Life in extreme environments, such as Arctic and Antarctic regions, is dominated by psychrophilic and psychrotrophic microorganisms (Morita, 1975). Psychrophilic bacteria have been able to colonize permanently the cold habitats according to their ability to cope with low temperature challenges. Their surviving strategies span from the preservation of the accurate balance of the cell-membrane fluidity (Goodchild *et al.*, 2004) and production of antifreeze proteins to avoid ice-crystallization to the protein's adaptations granting the natural enzymatic processes involved in the cellular growth. While over the last decades extremophilic enzymes have raised the interest to understand their structural adaptation features correlated with a high

---

<sup>1</sup> Department of Microbiology, Institute of Biology, 296 Splaiul Independentei, 060031 Bucharest, Romania

stability and activity at low temperatures to exploit their biotechnological potential (Cavicchioli *et al.*, 2011), several studies focused on structure-function characterization of both applicative-related catalysts and highly conserved key enzymes from extremophiles.

The *de novo* pyrimidine nucleotides biosynthesis has been characterized as a “universal process” (O’Donovan and Neuhard, 1970) being virtually found in all organisms belonging to Prokaryotes (Hutson and Downing, 1968), Archaea (Durbecq *et al.*, 1997) Eukaryotes (Denis-Duphil, 1989) and Mammals (Tatibana and Ito, 1969). The aspartate transcarbamoylase (ATCase, E.C. 2.1.3.2), a key enzyme of the pyrimidine biosynthetic pathway, has been extensively characterized in the case of the mesophilic bacterium *Escherichia coli* (Lipscomb and Stevens, 1990; Allewell, 1989; Hervé *et al.*, 1990; Helmstaedt *et al.*, 2001; Kantrowitz, 2012). All ATCases contain homotrimeric catalytic subunits composed of three identical catalytic chains PyrB of 33 kDa encoded by the *pyrB* gene (Weber, 1968). However, the quaternary structures of this enzyme from different organisms is highly variable, being composed of only catalytic trimers e.g. *Bacillus subtilis* (Potvin *et al.*, 1975) or forming multiprotein complexes with active dihydroorotase (DHOase) subunits in *Aquifex aeolicus* (Purcarea *et al.*, 2003) or inactive DHOase-like subunits in *Pseudomonas aeruginosa* (Vickrey *et al.*, 2002; Shurr *et al.*, 1995) replacing the regulatory subunits from the *E. coli* enzyme.

More recently, enzyme characterization of the hyperthermophilic homologues from *Pyrococcus abyssi* (Purcarea *et al.*, 1997), *Sulfolobus acidocaldarius* (Durbecq *et al.*, 1999) and *A. aeolicus* (Purcarea *et al.*, 2003) revealed structural adaptation to high temperatures. Meanwhile, little is known on ATCases from psychrophilic bacteria covering, to our knowledge only the enzymes from the Antarctic strain TAD1 (Sun *et al.*, 2005) and from *Moritella profunda* isolated from the deep Atlantic area (De Vos *et al.*, 2007). The crystal structure of the ATCase from the psychrophilic *M. profunda* showed a similar quaternary structure with that of *E. coli*, composed of 2 catalytic trimers and 3 regulatory dimers 2(c3):3(r2) but with a reduced thermal stability (De Vos *et al.*, 2005).

*Glaciibacter superstes* AHU1791 was isolated from an ice wedge in the Fox permafrost tunnel, Alaska, USA (64.952°N 147.617°W) (Katayama *et al.*, 2009). The phylogenetic analysis disclosed the strain AHU1791 as a genera affiliated to the Microbacteriaceae family. *G. superstes* is a gram-positive psychrophilic bacterium with a microscopic aspect of rod-shaped bacteria with a high G+C content (Katayama *et al.*, 2009).

In order to unravel the structural characteristics of cold-active ATCases allowing the initial step in pyrimidines biosynthesis at low temperatures, we conducted a comparative structural analysis of the putative enzyme from the psychrophilic bacterium *Glaciibacter superstes* with mesophilic and hyperthermophilic homologous enzymes.

## METHODS

Structural analyses were conducted in order to compare the ATCase amino acid sequence of the targeted psychrophilic bacterium (*G. superstes*) with the psychrophilic *Cryobacterium sp.* (Sequence ID: WP\_104166350.1), mesophilic *E. coli* (Sequence ID: 1Q95\_A) and hyperthermophilic *P. abyssi* (Sequence ID: WP\_010868442.1) homologues.

Primary structure analysis was achieved using ExPASy ProtParam software (Gasteiger *et al.*, 2005) in order to identify the protein amino acid composition (%), theoretical isoelectric point (pI), molecular weight (MW), extinction coefficient and a total of the positively and negatively charged residues.

The identity and similarity percentages between homologous enzymes were calculated from pair alignments of PyrB amino acid sequences using the Emboss Needle platform (Madeira *et al.*, 2019; [http://www.ebi.ac.uk/Tools/psa/emboss\\_needle/](http://www.ebi.ac.uk/Tools/psa/emboss_needle/)). Multiple sequence alignment of primary structures was performed using the CLUSTAL OMEGA EMBL-EBI 1.2.4 platform <http://www.ebi.ac.uk/Tools/msa/clustalo/> (Madeira *et al.*, 2019). Prediction of the secondary structure was obtained using the online CFSSP tool (Ashok Kumar, 2013). Protein hydrophobicity profile was modelled using Hydrophobic Cluster Analysis (HCA) 1.0.2 software of the RPBS Web Portal (<http://mobylye.rpbs.univ-paris-diderot.fr/cgi-bin/portal.py#forms::HCA>).

## RESULTS AND DISCUSSION

### Primary structure of the *G. superstes* ATCase

A screening of the *G. superstes* genome sequence (Katayama *et al.*, 2009) revealed the presence of a single *pyrB* gene (951 bp) coding for an ATCase catalytic chain (PyrB) of 317 amino acids (Table 1). The size of the *G. superstes* putative enzyme corresponded to a larger PyrB chain as compared to that of the mesophilic (*E. coli*) and hyperthermophilic (*P. abyssi*) homologous enzymes, indicating a shortening of the enzyme sequence at increasing environmental temperatures (Table 1). Meanwhile, a comparable size of PyrB was found in *Cryobacterium sp.*, a species also thriving at low temperatures.

Table 1

Size and calculated parameters of the ATCase PyrB catalytic chain from the psychrophilic, mesophilic and hyperthermophilic species

ATCase PyrB	Number of amino acids	Molecular weight	Theoretical pI	Aliphatic index
<i>G. superstes</i>	317	34092.64 Da	6.07	92.05
<i>Cryobacterium sp.</i>	316	34074.59 Da	6.56	92.41
<i>E. coli</i>	310	34296.17 Da	6.13	98.23
<i>P. abyssi</i>	308	34901.39 Da	6.29	103.77

The calculated molecular weight of the psychrophilic *G. superstes* PyrB chain (34.09 kDa) was lower than that of the mesophilic and hyperthermophilic counterparts, respectively (Table 1), indicating a temperature-dependant distribution of bulkier side chains residues in this enzyme. The overall structures of these proteins also varied with the environmental temperature of the host, showing increasing theoretical pI and aliphatic index values in the 6.07–6.29 and 92.05–103.77 ranges, respectively. However, the hydropathicity of the *G. superstes* ATCase showed an intermediate average value between those for the mesophilic and hyperthermophilic homologous enzymes.

The amino acid composition of the analysed enzymes showed a particular quantitative distribution in the case of the cold-active *G. superstes* ATCase (Table 2). The complete absence of cysteine residues appeared to be a distinctive pattern for the enzymes from psychrophilic bacteria. The lack of cysteines precludes the formation of disulfide bridges, thus conferring a higher flexibility to the enzyme. In addition, both enzymes showed a reduced content of glutamate and lysine residues and a higher representation of aspartate and arginine residues as compared to the mesophilic and hyperthermophilic homologs.

Table 2

Amino acid composition the ATCase catalytic subunit of *G. superstes*, *Cryobacterium sp.*, (Sequence ID: WP\_104166350.1), mesophilic *E. coli* (Sequence ID: IQ95\_A) and hyperthermophilic *P. abyssi* (Sequence ID: WP\_010868442.1).  
Total residue number and relative content (%)

PyrB amino acid composition	<i>G. superstes</i>		<i>Cryobacterium sp.</i>		<i>E. coli</i>		<i>P. abyssi</i>	
	Number	%	Number	%	Number	%	Number	%
<b>Ala (A)</b>	37	11.7	40	12.7	34	11.0	20	6.5
<b>Arg (R)</b>	26	8.2	27	8.5	15	4.8	21	6.8
<b>Asn (N)</b>	7	2.2	10	3.2	15	4.8	5	1.6
<b>Asp (D)</b>	28	8.8	24	7.6	21	6.8	17	5.5
<b>Cys (C)</b>	0	0.0	0	0.0	1	0.3	1	0.3
<b>Gln (Q)</b>	8	2.5	5	1.6	14	4.5	8	2.6
<b>Glu (E)</b>	12	3.8	13	4.1	14	4.5	31	10.1
<b>Gly (G)</b>	26	8.2	23	7.3	15	4.8	20	6.5
<b>His (H)</b>	8	2.5	10	3.2	11	3.5	8	2.6
<b>Ile (I)</b>	15	4.7	18	5.7	15	4.8	20	6.5
<b>Leu (L)</b>	31	9.8	31	9.8	38	12.3	36	11.7
<b>Lys (K)</b>	10	3.2	8	2.5	15	4.8	24	7.8
<b>Met (M)</b>	9	2.8	9	2.8	8	2.6	6	1.9
<b>Phe (F)</b>	9	2.8	9	2.8	12	3.9	10	3.2

Table 2 (continued)

<b>Pro (P)</b>	12	3.8	12	3.8	12	3.9	11	3.6
<b>Ser (S)</b>	25	7.9	30	9.5	20	6.5	13	4.2
<b>Thr (T)</b>	22	6.9	19	6.0	18	5.8	18	5.8
<b>Trp (W)</b>	4	1.3	4	1.3	2	0.6	1	0.3
<b>Tyr (Y)</b>	2	0.6	3	0.9	8	2.6	10	3.2
<b>Val (V)</b>	26	8.2	21	6.6	22	7.1	28	9.1
<b>Pyl (O)</b>	0	0.0	0	0.0	0	0.0	0	0.0
<b>Sec (U)</b>	0	0.0	0	0.0	0	0.0	0	0.0

Protein stability associated to formation of salt bridges was evaluated on the arginine and lysine residues content (Gurry *et al.*, 2010). Thus, an increased protein flexibility was corroborated with the formation of salt bridges due to ionic interactions between Lys and Arg. For the analysed PyrB sequences, the calculated Arg/Lys ratio (Table 3) showed a temperature-dependent variation.

Table 3

Arginine / Lysine residues number ratio in various ATCases. A ratio score closer to unit indicates a lower probability for salt bridges formation

	<b>Arg (R)/(Arg (R) + Lys (K))</b>
<i>G. superstes</i>	0.7222
<i>Cryobacterium sp.</i>	0.7714
<i>E. coli</i>	0.5000
<i>P. abyssi</i>	0.4667

The high ratio (0.7222–0.7714) between the number of Arg and Lys residues in both cold-adapted enzymes *G. superstes* and *Cryobacterium sp.* indicated a lower presence of ionic interactions leading to a reduced number of salt bridges as compared to the mesophilic and hyperthermophilic ATCases. The lower ratios calculated for the *E. coli* and *P. abyssi* enzymes showed a higher content of salt bridges in the mesophilic and hyperthermophilic ATCases which could be required to maintain the 3D structure and prevent thermal denaturation at higher temperatures. Previous hypothesis also corroborates the reduced occurrence of salt bridges in the psychrophilic bacteria where low temperature have the opposite effect (Hendsch *et al.*, 1994).

While the number of individual amino acids arginine, lysine, aspartate and glutamate was highly different in ATCases from the psychrophilic, mesophilic and

hyperthermophilic species (Table 2), only slight variations in the occurrence of collective positively charged residues (Arg+Lys) and negatively charged residues (Asp+Glu) was observed between these enzymes adapted to different thermal conditions (Table 4).

Table 4

Charged residues content of the psychrophilic, mesophilic and hyperthermophilic bacterial ATCases

ATCase (PyrB chain)	Total number of negatively charged residues (Asp + Glu)	Total number of positively charged residues (Arg + Lys)
<i>G. superstes</i>	40	36
<i>Cryobacterium sp.</i>	37	35
<i>E. coli</i>	35	30
<i>P. abyssi</i>	48	45

In this case, the higher number of Asp+ Glu and Arg + Lys in *G. superstes* ATCase as compared to the *E. coli* enzyme, but lower than the *P. abyssi* amino acid chain, suggested enhanced ionic interactions relative to the mesophilic host enzyme but lower interactions than the hyperthermophilic one, confirming that extremophilic enzymes could adopt different strategies for thermal adaptation. Pair alignment of the microbial PyrB sequences (Table 5) that the *G. superstes* ATCase is homologous to the corresponding enzyme from the psychrophilic *Cryobacterium sp.*, showing high identity (88%) and similarity (92%) scores. Interestingly, the cold-active enzyme showed a very low conservation of the primary structure with the mesophilic and hyperthermophilic counterparts, with comparable identity (30.0–32.7%) and similarity scores (47.8–50.3%). This result suggested shared adaptations mechanisms to the extreme environment which could have originated from a common mesophilic enzyme with a consequent revision of the protein structures to endure the harsh environmental conditions.

Table 5

Identity and similarity scores between *G. superstes* ATCase and corresponding enzymes from the psychrophilic *Cryobacterium sp.*, the mesophilic *E. coli* and the hyperthermophilic *P. abyssi*

		<i>Cryobacterium sp.</i>	<i>E. coli</i>	<i>P. abyssi</i>
<i>G. superstes</i> ATCase PyrB	Identity (%)	88.0	30.0	32.7
	Similarity (%)	92.0	47.8	50.3



The interface C1-C4 between the catalytic trimmers (Fig. 1) was also partially affected by the non-conservative substitutions Lys171→Leu, Tyr172→His, Asp276→Leu contributing to a higher hydrophobicity of the interface as compared with that in the mesophilic ATCase (Fig. 1).

Several substitutions were also observed of the residues forming the interface CP-ASP between the carbamoyl phosphate and aspartate binding domains (Fig. 1) introducing polar and charged residues (Ile7→Thr, Gln33→Glu), bulkier hydrophobic side chain (Gln81→Trp), and increasing flexibility by substitution of a charge residue with glycine (Asp87→Gly) in the psychrophilic enzyme relative to the mesophilic homologue.

Comparison of the secondary structure (Fig. 2; Table 6) indicated a variable composition and distribution of helices, turns and sheets along the analysed ATCases not strictly related to the species growth temperature, while depicted a higher content of coils in the amino acid sequence belonging to the psychrophilic *G. superstes* enzyme. The helix and turn contents were comparable to those of the psychrophilic *Cryobacterium sp.* enzyme, while the sheet composition is similar to the mesophilic *E. coli* ATCase (Table 6). Temperature-dependent secondary structure could only address the turn content, with a strong decrease from the cold-active ATCases (7.6%–8.8%) to the hyperthermophilic *P. abyssi* enzyme (2.9%). Interestingly, the *G. superstes* PyrB coil structures content was 2-fold higher than that in the mesophilic *E. coli*, and 5-fold higher than in both the *P. abyssi* and *Cryobacterium sp.* enzymes (Table 6) suggesting that their position (Fig. 2) could play a critical role in the protein folding and flexibility in order to adapt the catalytic process to extremely low temperatures. The highest abundance of coils in the secondary structure of *G. superstes* could be responsible for enhanced protein-protein interactions allowing a more flexible catalytic process at low temperatures. Also, the *G. superstes* ATCase extended 80's and 240's loops as compared to the mesophilic and hyperthermophilic homologous enzymes (Fig. 2) could contribute to a putative cooperative effect of the substrates binding at low temperatures, considering that these flexible loops play a major role in the T→R transition of the quaternary structure during catalysis (Kantrowitz, 2012).

Table 6

Composition of the secondary structure elements in ATCase from different species

ATCase PyrB chain	Secondary structure composition			
	Helix (%)	Sheet (%)	Turn (%)	Coil (%)
<i>G. superstes</i>	50.8	21.5	7.6	20.2
<i>Cryobacterium sp.</i>	49.5	32.2	8.8	9.5
<i>E. coli</i>	59.7	23.9	6.1	10.3
<i>P. abyssi</i>	54.9	37.7	2.9	4.5

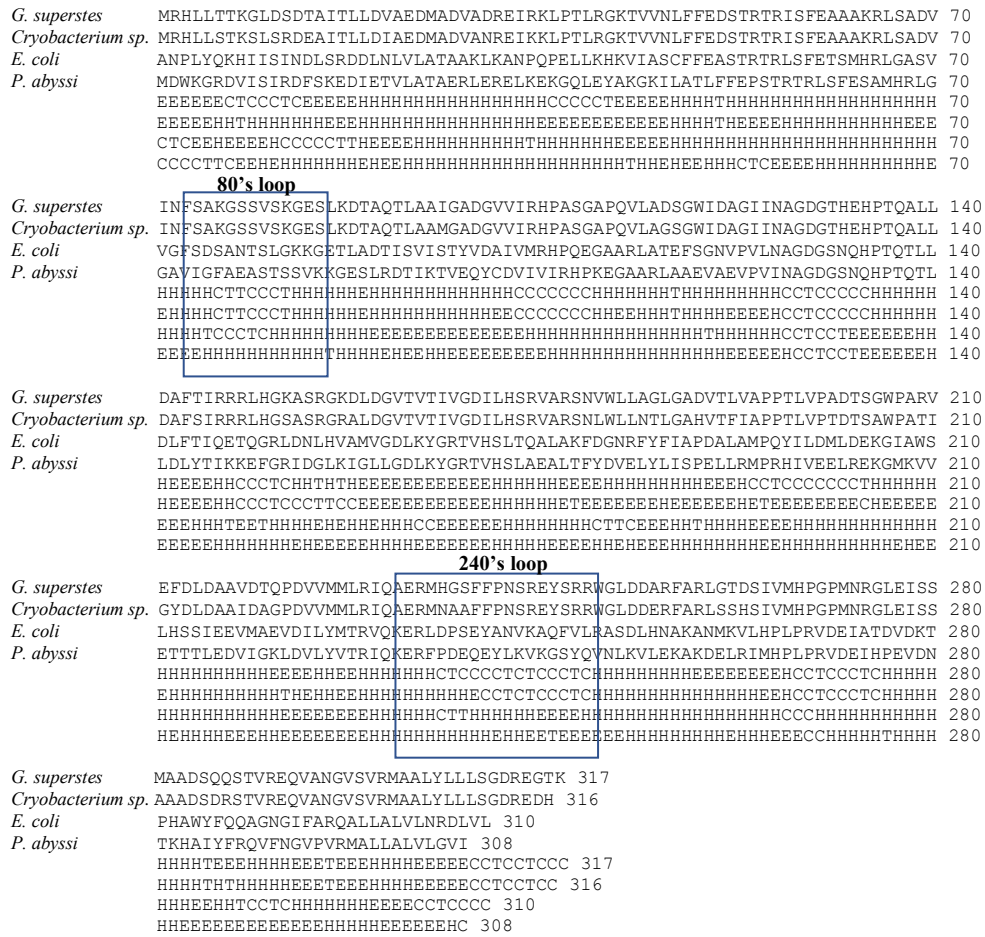


Fig. 2. Secondary structure alignment of *G. superstes*, *Cryobacterium sp.*, *E. coli* and *P. abyssi* ATCase PyrB catalytic chain. H= Helix; E= Sheet; T=Turn; C= Coil.

Modelling of the hydrophobic cores' distribution within ATCase catalytic chain sequences allowed the comparison of the hydrophobic clusters profile of psychrophilic, mesophilic and hyperthermophilic homologous enzymes (Fig. 3). For both cryophilic species, reduced hydrophobic clusters were present along the carbamoyl phosphate (CP) domain (residues 1-154) unlike the hyperthermophilic enzyme (Fig. 3). This could be related to the very low stability of this substrate at high temperatures, requiring the direct transfer (channeling) facilitated by a hydrophobic structure from the previous enzyme where it is synthesized without being released in the cell (Purcarea *et al.*, 1999), a strategy that is not necessary in cold-adapted enzymes functioning at low temperatures. Moreover, a reduced hydrophobicity was also visible in the CP-Asp link region (residues 194-203) of the two analysed psychrophilic enzymes (Fig. 3) relative to both mesophilic and hyperthermophilic

ATCases, with possible contribution to an enhanced chain flexibility for the domains closure during catalysis (Wang *et al.*, 2007).

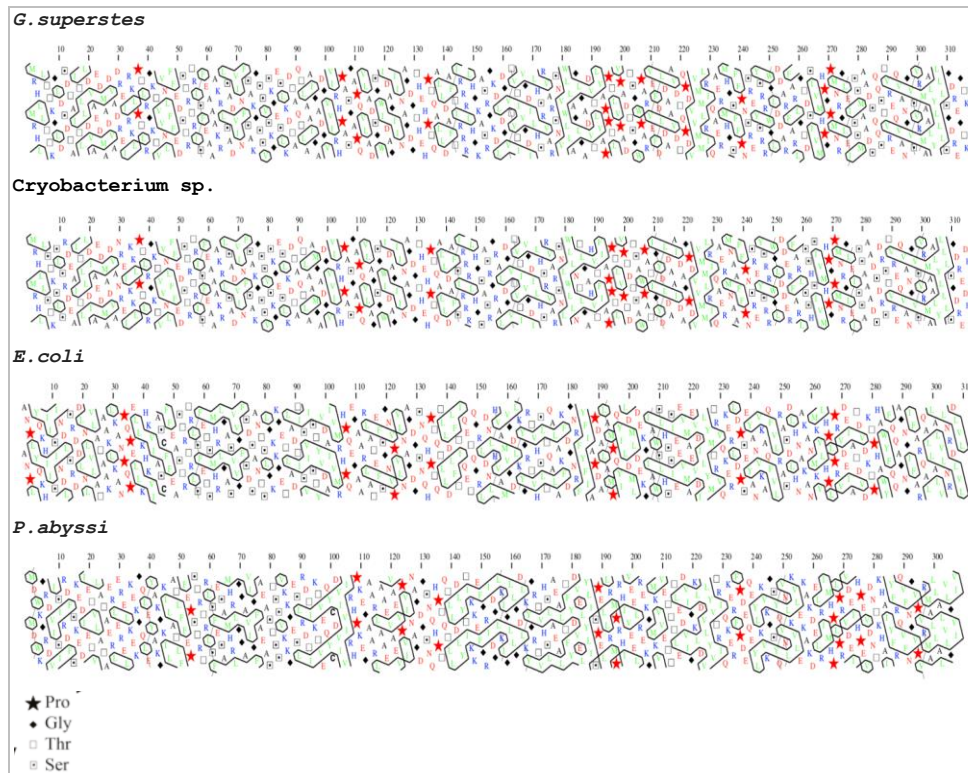


Fig. 3. Hydrophobic cluster analysis of ATCase PyrB sequences from different species.

## CONCLUSION

The current structural investigation of the ATCase from the psychrophilic bacterium *G. superstes* contributes to a better understanding of cold adaptation mechanisms by highlighting a series of molecular features favouring catalysis at low temperatures in one of the key enzymes involved in DNA synthesis, responsible for the cell resilience in bacteria thriving in frozen environments.

The primary structure emphasized a full conservation of the active site residues found in ATCases from the psychrophilic *Cryobacterium sp.*, the mesophilic *E. coli* and hyperthermophilic *P. abyssi*, in accordance with the ubiquity of the enzyme and the common reaction catalyzed by this enzyme in all organisms. Interestingly, the ATCase from the psychrophilic bacterium showed higher identity and similarity

scores with the hyperthermophilic counterpart suggesting, allegedly, common adaptations to extreme environments. However, the secondary structure and hydrophobic cores distribution are highly different from those of the *E. coli* and *P. abyssi* ATCases. These patterns appear to favor a higher solubility and an increased flexibility to this psychrophilic protein that could reduce the activation energy of the catalytic reaction by reducing the distance between the substrates binding site residues (Helmstaedt *et al.*, 2001). Solving the x-ray crystallographic structure of this ATCase will help unravelling further molecular adaptations of this enzyme to low temperatures in comparison to mesophilic and (hyper)thermophilic counterparts, in order to extend the general understanding of the structural strategies of key catalysts from extremophiles adapted to cold environments. This study will help understanding not only the adaptation mechanisms to extreme environmental conditions of this class of enzymes, but could also contribute to shedding light on the identification of novel ATCase inhibitors used for development of anticancer drugs.

### Acknowledgements

This study was financially supported by the RO1567-IBB05/2019 grant and the European Union's Horizon 2020 Research and Innovation Programme under the Marie Skłodowska-Curie grant agreement No 675546.

### REFERENCES

1. Allewell N.M., 1989, Escherichia Coli Aspartate Transcarbamoylase: Structure, Energetics, and Catalytic and Regulatory Mechanisms. *Annual Review of Biophysics and Biophysical Chemistry*. **18**, pp. 71–92. Doi:10.1146/annurev.bb.18.060189.00044
2. De Vos D. *et al.*, 2007 Structural Investigation of Cold Activity and Regulation of Aspartate Carbamoyltransferase from the Extreme Psychrophilic Bacterium *Moritella profunda*. *Journal of Molecular Biology*. **365**, pp. 379–395. Doi:10.1016/j.jmb.2006.09.064
3. De Vos D. *et al.*, 2005 Expression, purification, crystallization and preliminary X-ray crystallographic studies of a cold-adapted aspartate carbamoyltransferase from *Moritella profunda*. *Acta Crystallographica Section F*. **61**, pp. 279–281. Doi:10.1107/S174430910500285X
4. Denis-Duphil M., 1989, Pyrimidine biosynthesis in *Saccharomyces cerevisiae*: the *ura2* cluster gene, its multifunctional enzyme product, and other structural or regulatory genes involved in de novo UMP synthesis. *Biochemistry and Cell Biology*. **167**, 612–31.
5. Durbecq V. *et al.*, 1997, The carbamate kinase- like carbamoyl phosphate synthetase of the hyperthermophilic archaeon *Pyrococcus furiosus*, a missing link in the evolution of carbamoyl phosphate biosynthesis. *Proceedings of the National Academy of Sciences of the United States of America*. **94**, pp. 12803–12808.
6. Gasteiger E. *et al.*, 2005, Protein identification and analysis tools on the Expasy Server; in John M. Walker (ed): *The Proteomics Protocols Handbook*, Humana Press. pp. 571–607.
7. Goodchild A. *et al.*, 2004, A proteomic determination of cold adaptation in the Antarctic archaeon, *Methanococcoides burtonii*. *Molecular Microbiology*. **53**, pp. 309–321. Doi:10.1111/j.1365-2958.2004.04130.x
8. Gurry T. *et al.*, 2010, The contribution of interchain salt bridges to triple-helical stability in collagen. *Biophysical Journal*. **98**, pp. 2634–2643. Doi:10.1016/j.bpj.2010.01.065

9. Helmstaedt K. *et al.*, 2001, Allosteric regulation of catalytic activity: *Escherichia coli* aspartate transcarbamoylase versus yeast chorismate mutase. *Microbiology and Molecular Biology Reviews*. **65**, pp. 404–421. Doi:10.1128/MMBR.65.3.404-421.2001
10. Hendsch Z.S. and B. Tidor, 1994, Do salt bridges stabilize proteins? A continuum electrostatic analysis. *Protein Science*. **3**, pp. 211–226. Doi:10.1002/pro.5560030206
11. Hervé G. *et al.*, 1990, Engineering aspartate transcarbamoylase. *Biochimie*. **72**, pp. 609–616.
12. Hutson J.Y., and M. Downing, 1968, Pyrimidine biosynthesis in *Lactobacillus leichmannii*. *Journal of Bacteriology*. **96**, pp. 1249–1254.
13. Jones M. *et al.*, 1955, Carbamyl phosphate, the carbamyl donor in enzymatic citrulline synthesis. *Journal of the American Chemical Society*. **77**, 819–820.
14. Kantrowitz E.R., 2012, Allostery and cooperativity in *Escherichia coli* aspartate transcarbamoylase. *Archives of Biochemistry and Biophysics*. **519**, pp. 81–90.
15. Katayama T., 2009, *Glaciibacter superstes* gen. nov., sp. nov., a novel member of the family Microbacteriaceae isolated from a permafrost ice wedge. *International Journal of Systematic and Evolutionary Microbiology*. **59**, pp. 482–486. Doi: 10.1099/ij.s.0.001354-0
16. Ke H.W.N. *et al.*, 1988, Complex of *N*-phosphonacetyl-L-aspartate with aspartate carbamoyltransferase from *Escherichia coli*. *Journal of Molecular Biology*. **204**, pp. 725–747 Doi:10.1016/0022-2836(88)90365-8
17. Lipscomb W.N. and R.C. Stevens, 1990, Allosteric control of quaternary states in *E. coli* aspartate transcarbamoylase. *Biochemical and Biophysical Research Communications*. **171**, pp. 1312–1318.
18. Madeira F. *et al.*, 2019, The EMBL-EBI search and sequence analysis tools APIs in 2019. *Nucleic Acids Research*. Doi: <https://doi.org/10.1093/nar/gkz268>
19. Moffatt B.A. and H. Ashihara, 2002, Purine and pyrimidine nucleotide synthesis and metabolism. *The arabidopsis book*, **1**, e0018. Doi:10.1199/tab.0018
20. Morita R.Y., 1975, Psychrophilic bacteria. *Bacteriology Reviews*. **39**, pp. 144–167.
21. O'Donovan G. and J. Neuhard, 1970, Pyrimidine metabolism in Microorganisms. *Bacteriology Reviews*. **34**, pp. 278–343.
22. Potvin B.W. *et al.*, 1975, Pyrimidine biosynthetic pathway of *Bacillus subtilis*. *Journal of Bacteriology*. **123**, pp. 604–615.
23. Purcarea C. *et al.*, 2003, Aquifex aeolicus Aspartate Transcarbamoylase, an Enzyme Specialized for the Efficient Utilization of Unstable Carbamoyl Phosphate at Elevated Temperature. *Journal of Biological Chemistry*. **278**, pp. 52924–52934. Doi:10.1074/jbc.m309383200
24. Purcarea C. *et al.*, 1999, Channeling of Carbamoyl Phosphate to the Pyrimidine and Arginine Biosynthetic Pathways in the Deep Sea Hyperthermophilic Archaeon *Pyrococcus abyssi*. *Journal of Biological Chemistry*. **274**, pp. 6122–6129. Doi:10.1074/jbc.274.10.6122
25. Purcarea C. *et al.*, 1997, Aspartate transcarbamoylase from the deep-sea hyperthermophilic archaeon *Pyrococcus abyssi*: genetic organization, structure, and expression in *Escherichia coli*. *Journal of bacteriology*. **179**, pp. 4143–4157. Doi:10.1128/jb.179.13.4143-4157.1997
26. Schurr M.J. *et al.*, 1995, Aspartate transcarbamoylase genes of *Pseudomonas putida*: requirement for an inactive dihydroorotase for assembly into the dodecameric holoenzyme. *Journal of Bacteriology*. **177**, pp. 1751–1759.
27. Sun K. *et al.*, 1998, Properties of aspartate transcarbamoylase from *TAD1*, a psychrophilic bacterial strain isolated from Antarctica. *FEMS Microbiology Letters*. **164**, pp. 375–382. Doi:10.1111/j.1574-6968.1998.tb13112.x
28. Tatibana M. and J. Ito, 1969, Control of pyrimidine biosynthesis in mammalian tissues. I. Partial purification and characterization of glutamine utilizing carbamyl phosphate synthetase of mouse spleen and its tissue distribution. *Journal of Biological Chemistry*. **244**, pp. 5403–5413.
29. Vickrey J.F. *et al.*, 2002, *Pseudomonas aeruginosa* Aspartate Transcarbamoylase Characterization of its catalytic and regulatory properties. *Journal of Biological Chemistry*. **277**, pp. 24490–24498.
30. Wang J. *et al.*, 2007, Structural model of the R state of *Escherichia coli* aspartate transcarbamoylase with substrates bound. *Journal of Molecular Biology*, **371**, pp. 1261–1273. Doi:10.1016/j.jmb.2007.06.011
31. Weber K., 1968, New Structural Model of *E. coli* Aspartate Transcarbamoylase and the Amino-acid Sequence of the Regulatory Polypeptide Chain. *Nature*. **218**, pp. 1116–1119.